



PERGAMON

Available online at [www.sciencedirect.com](http://www.sciencedirect.com)

SCIENCE @ DIRECT®

International Journal of Rock Mechanics & Mining Sciences 40 (2003) 1089–1097

International Journal of  
Rock Mechanics  
and Mining Sciences

[www.elsevier.com/locate/ijrmms](http://www.elsevier.com/locate/ijrmms)

# Enhancing rock stress understanding through numerical analysis

R. Hart\*

*Itasca Consulting Group Inc., 111 3rd Ave. S., Suite 450, Minneapolis, MN 55401, USA*

Accepted 10 July 2003

## Abstract

Numerical analysis provides a useful tool to enhance the understanding of rock stress. This paper presents several applications of numerical analysis to evaluate the influence of different factors, such as topology, excavation, loading history and geologic structure, on the state of stress in rock. The discussion focuses on the numerical technique known as the explicit, dynamic solution scheme, and describes how this scheme is well suited to simulate these factors. Recent advances with the explicit solution method are also presented, including the correlation of this method to acoustic and microseismic data to determine stress state information. Future development involves the extension of three-dimensional explicit solution models to simulate large-scale regions of a rock mass. An approach to this development is outlined.

© 2003 Elsevier Ltd. All rights reserved.

## 1. Introduction

In all civil or mining engineering projects, there is an in situ state of stress in the ground before any excavation or construction is started. It is important in the development of a numerical model for a rock engineering analysis to reproduce this in situ state as closely as possible, because the stress state can influence the results of the analysis both in terms of the assessment of stability and the calculation of the deformation state. Ideally, information about the initial stress state comes from field measurements but, when these are not available, the model can still be developed for a range of possible conditions. Although this range is potentially infinite, there are a number of constraining factors (e.g. the system must be in equilibrium, and the chosen yield criteria must not be violated anywhere).

It is important to consider the conditions that can influence the state of stress and then assess the capability of the numerical method to represent these conditions in the model. Conditions include the three-dimensionality of the problem geometry, the presence of inhomogeneities and discontinuous features in the rock mass, and the loading history of the rock mass. For example, irregular surface topology, repeated tectonic movements, material failure, overburden removal, and

locked-in stresses due to faulting and localization can produce a complex in situ state of stress even before excavation-induced stresses are imposed.

Several different numerical schemes have been used to represent in situ state of stress in rock engineering models. For a general discussion on advantages and current limitations of numerical models used in rock engineering, see [1]. This discussion focuses on one type of method, the *explicit, dynamic solution scheme*, which is considered well suited to represent several of the conditions affecting an in situ stress state in a numerical analysis. The capabilities of this method are described below. The application of the explicit, dynamic solution method in progressively more complicated situations is then presented in order to illustrate procedures for representing stress conditions in a rock engineering model and for checking the reliability of the stress predictions.

## 2. Explicit, dynamic solution scheme

The explicit, dynamic solution scheme provides the means to follow, in a realistic manner, the complete evolution of geologic systems. The method can simulate physical instability and path dependence, and allows the implementation of extremely nonlinear constitutive models—such as strain-softening material models or brittle-breakage contact models.

\*Tel.: +1-612-371-4711, fax: +1-612-371-4717.

E-mail address: [rhart@itascacg.com](mailto:rhart@itascacg.com) (R. Hart).

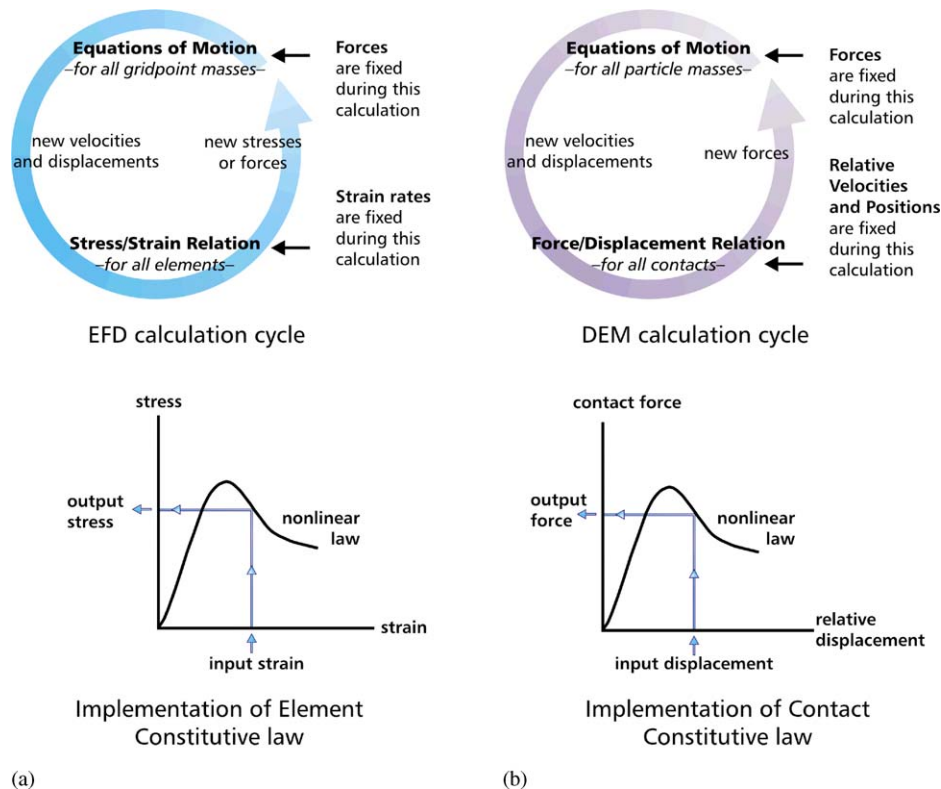


Fig. 1. Components of the explicit, dynamic solution scheme: (a) explicit finite difference method; and (b) distinct element method.

The method applies for both quasi-static and fully dynamic systems. Every derivative in the set of governing equations is replaced directly by an algebraic expression written in terms of field variables (e.g. stress or force and displacement) at discrete points in space. Using the complete dynamic equations ensures that the numerical scheme is stable when the physical system being modeled is unstable.

The explicit calculation cycle solves two sets of equations: motion and constitutive. The equation components are illustrated in Fig. 1. In both sets, variables on the right-hand side of expressions are known and can be regarded as fixed for the duration of a calculation step. Consequently, each element in this type of model appears to be physically isolated from its neighbors during one calculation step. Thus, nonlinear constitutive relations are implemented without difficulty, because only local conditions are relevant during the calculation step. No iterations are necessary to follow nonlinear laws, and no matrices are formed.

The solution scheme applies equally well for both continuum and discontinuum numerical models. For continuum models, the motion and constitutive equations are formulated in terms of stresses and strain increments within elements in a continuum grid; for discontinuum models, the equations are formulated in terms of forces and displacements at contacts in a discrete particulate system. In continuum models, the scheme is implemented as an explicit finite-difference

(EFD) formulation (Fig. 1a). In discontinuum models, the discrete, or distinct, element method (DEM) embodies the explicit, dynamic scheme (Fig. 1b). For details on the explicit, dynamic solution scheme as developed for EFD continuum models, see [2]; for DEM discontinuum models, see [3].

The explicit, dynamic approach is neither new nor unique; it has been used successfully on many ill-behaved systems over the past 30 years. For example, see [4,5] for early applications. The commercial codes FLAC [6] and FLAC3D [7] are examples of continuum numerical programs based on the EFD formulation. The particle codes PFC2D [8] and PFC3D [9] are example discontinuum programs based on the DEM solution scheme. The discontinuum programs for modeling jointed rock, UDEC [10] and 3DEC [11], use the DEM scheme to simulate motion at joint contacts between rock blocks and the EFD formulation to simulate deformation with the blocks. Applications of both the EFD and DEM approaches to represent stress conditions are illustrated in the following sections.

### 3. Influence of surface topology, excavations and loading history on stress state

The simplest approach to represent an in situ stress state in a numerical model is to assume the vertical stresses are gravitationally induced and that there is a

natural ratio between horizontal and vertical stress given by  $\nu/(1 - \nu)$ , where  $\nu$  is the Poisson's ratio. This formula is derived from the assumption that gravity is applied suddenly to a mass of elastic material in which lateral movement is prevented. This condition hardly ever applies in practice, due to the various effects on the stress state, as discussed previously.

If the history of a particular volume of material is known, it is possible to simulate this whole process numerically to arrive at the initial conditions for a planned engineering work. However, this approach usually is not feasible.

Typically, a compromise is made in which a set of stresses is installed in the model and then an equilibrium state is calculated. There are an infinite number of equilibrium states for a given system. Each state will produce a different, but physically valid, stress distribution. Some common ways to produce an equilibrium state are:

1. to not initialize the stresses in the model, but allow gravitational loading to compact the model;
2. to initialize the horizontal stress only before applying gravitational loading;
3. to impose a constant stress at the lateral boundaries of the model rather than a zero horizontal displacement;
4. to remove the irregular overburden from the initial model of uniform thickness, then apply the overburden after the initial equilibrium state is reached;
5. to allow plastic flow of the material to occur, thus removing stress concentrations; and
6. to build up the profile layer by layer and equilibrate each layer.

The method selected should attempt to approximate the type of geological processes that are believed to have occurred in the field.

If stress measurements are available, then the equilibrium stress state in the model should be checked by comparison to the field measurements. One difficulty with comparing field measurements is that it is not always possible to perform in situ stress measurements sufficiently far from underground excavations to determine the virgin (pre-excavation) stress state. This is particularly true for mines using massive mining methods.

Numerical modeling can be used to quantify the various forms of induced stresses, such as those generated by topology, excavations or material property variations. The virgin stress field can then be computed by subtracting the induced stresses generated by the excavations from the total or measured stresses. In this way, it is possible to use stress measurements, which are known to include induced stresses from various sources, to check the model stress state.

A procedure to estimate the virgin stresses from in situ measurements is described as follows. See [12] for a more thorough explanation of this procedure. The procedure is based on the assumption that the total stress field can be evaluated by considering the vertical component and horizontal component separately. The vertical stresses are considered to be primarily gravitational in origin. The horizontal stresses are considered to include both gravitational and tectonic stress components. Tectonic stresses are assumed to include all stresses induced by nongravitational effects. For this procedure, it is also assumed that the stresses in the far field (i.e. sufficiently removed the effects of excavations) are principal stresses. These are the stresses applied at the model boundaries.

The total measured stress field,  $\sigma_{ij}^{\text{meas}}$ , is decomposed into two components: a gravitational stress component,  $\sigma_{ij}^{\text{grav}}$ , and a tectonic stress component,  $\sigma_{ij}^{\text{tect}}$ . The gravitational stress is determined from the numerical model developed on the basis of the known topology, excavation geometry and material unit weights. An elastic analysis is performed to determine the gravitational stress state (with other factors neglected). Then, by knowing both  $\sigma_{ij}^{\text{meas}}$  and  $\sigma_{ij}^{\text{grav}}$ , the tectonic stress tensor can be calculated from

$$\sigma_{ij}^{\text{tect}} = \sigma_{ij}^{\text{meas}} - \sigma_{ij}^{\text{grav}}. \quad (1)$$

The resultant calculated vertical stresses from the gravitational-loading analysis are compared to the corresponding measured vertical stresses, and all measured stress components are scaled to bring the measured vertical stress into agreement with the calculated vertical stress. If the computed and measured vertical components of stress are found to differ by a large amount, then either the model is incorrect (such as having incorrect densities), there are unknown sources of induced stress (such as locked-in stresses from geological processes, as discussed in the next section), or there are significant errors in the measurements. In this situation, it is wise to investigate further the reason for the stress anomaly.

The unknown tectonic stress components are determined by applying unit tractions to the boundaries of the model and computing the stresses induced at points within the model corresponding to the measurement points. The correct “far-field” tectonic boundary stresses then are computed by scaling the unit stress results to match the magnitudes of the components obtained using Eq. (1). Thus, the total far-field stress state is taken as the combination of the corrected horizontal tectonic stresses applied at the model boundary plus the gravitational stresses.

The pre-excavation, virgin stress state is determined finally by performing a numerical analysis with “filled-in” excavated regions in the model. The excavation-induced stresses can then be found by subtracting the

virgin stress at any point from the total (post-excavation) stress.

This procedure can involve several simulations to calibrate the model with the measured stresses. McKinnon [12] describes a tensor-fitting technique to assist with comparing tectonic stresses from the numerical analysis to those of the measured stress field. The procedure has been used successfully on several different projects. For example, see [13] for an example calibration of a 3DEC model for the in situ stress field at the Wellenberg low- and intermediate-level nuclear repository site in Germany. Fig. 2 shows the model developed for the site. Fig. 3 illustrates a FLAC3D model, under development, representing the initial regional stress field

at the high-level nuclear repository site at Yucca Mountain in the USA [14]. Other cases are described by McKinnon and Lorig [15]. Although three-dimensional models are generally required, it is possible, in certain cases, to evaluate the stress state with this approach based on two-dimensional models; e.g. see [16,17].

The numerical model in this procedure needs to incorporate the irregular geometry of the topography and excavations accurately, but it typically assumes simplifying behavior (homogeneous, isotropic, linear elastic) for the rock masses. However, in many instances, it is necessary to include the effect of the tectonic loading history and the influence of inhomogeneities,

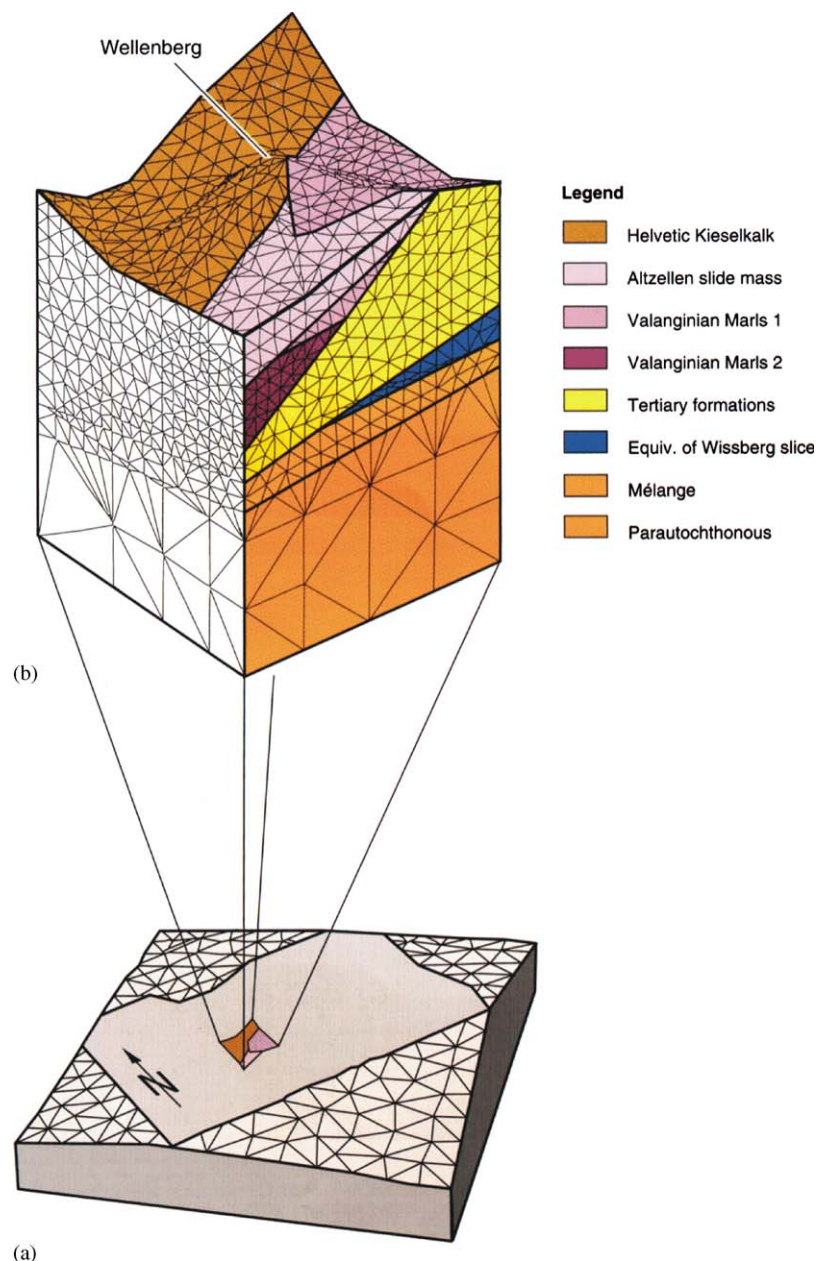


Fig. 2. 3DEC model for an in situ stress field at the Wellenberg site (from [13]): (a) full model; and (b) region of interest view of rock mass types.



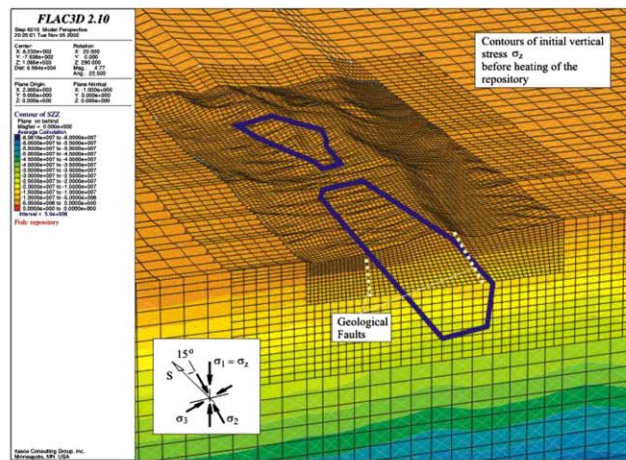
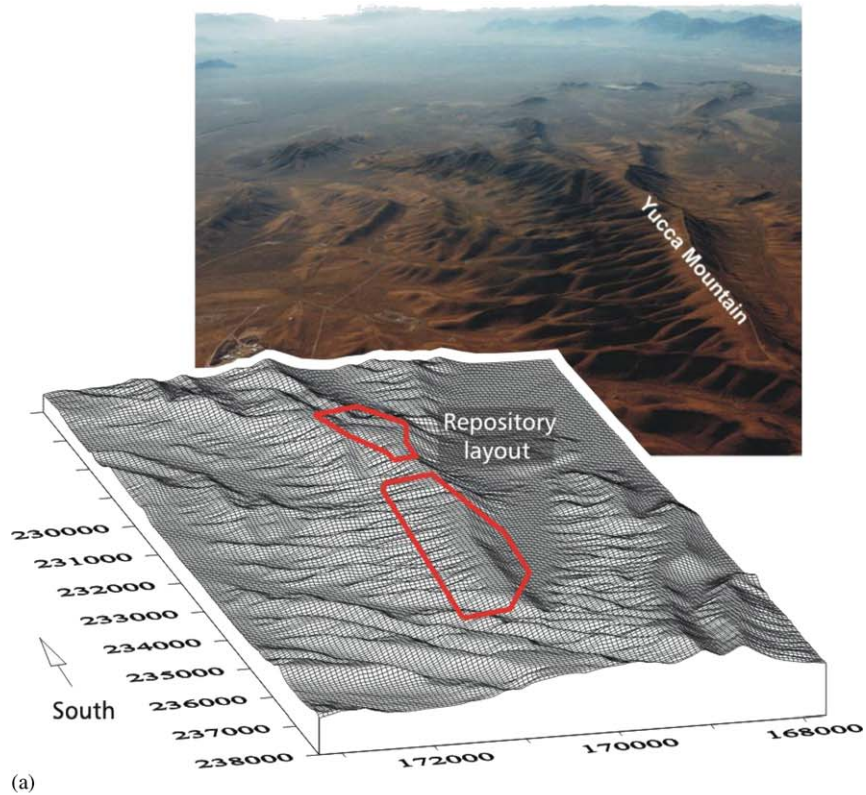


Fig. 3. FLAC3D model of Yucca Mountain site (from [14]): (a) Yucca Mountain topological setting; and (b) FLAC3D model—vertical stress contours for gravitational loading.

discontinuities and other geological features as potential sources of local distortions to the stress field. The advantage of using the explicit, dynamic solution scheme is that the loading history and the nonlinear effects of geologic structures can be added directly to the model. This is discussed in the following section.

#### 4. Influence of geologic structure on stress state

A spatial heterogeneity in the initial stress state can develop in a rock mass due to the presence of geologic structures such as joints, fractures and faults. This results from both the stress path followed during the geologic history of the medium and the physical

processes (related to fracturing and slip and separation along discontinuities) that may have occurred at different stages in the history.

For example, natural stress concentrations are inferred from stress measurements to be located in proximity to major discontinuities in a rock mass (e.g. [18]). These heterogeneities in the stress field may be attributed to irrecoverable movements induced along existing joint planes during cycles of regional tectonic activity. The local stress heterogeneities effectively are “locked-in” by the prior tectonic activity.

The nature of the stress concentrations can be understood by considering a single finite-length fracture subjected to a uniform shear stress along the crack surface. Knott [19] provides the exact solution for the stress concentration that develops around the crack tip for this case, assuming a constant normal stress along the crack and a limiting friction coefficient,  $\mu$ , for the fracture. The solution indicates that the stress concentration can extend transversely to the crack to a distance of approximately the half-width of the crack.

Brady et al. [20] demonstrated that, in a multi-jointed medium, the area of the stress concentration can be influenced by the presence of neighboring cracks. Fig. 4 shows one jointing pattern studied in their work. A UDEC model of this pattern was subjected to a load cycle beginning at an isotropic stress state, then increasing the major-to-minor principal stress ratio to 4:1, with the major principal axes oriented  $30^\circ$  to the  $x$ -axis, and finally returning to the isotropic state. When the stress ratio is increased, slip occurs along some of the

joints in the interior of the model. Fig. 5 plots contours of  $\sigma_{xx}$  after completion of the load cycle. The plot indicates the development of stress concentrations resulting from the joint slippage. The localized stress heterogeneities that are locked-in after the original isotropic far-field stresses are restored are a consequence of these stress concentrations that develop at the endpoints of the discontinuous joints in the model.

Geostatistical analysis of stress data generated from these jointed models suggests that the stresses calculated at points in the models at spacings less than the mean joint spacings may be biased and not representative of the overall mean stress. This confirms the influence the geologic structure can have in determining the stress distribution. Further, this study shows the role numerical models can take in helping develop guidelines for establishing representative numbers and locations of stress measurement sites in order to provide a reliable estimate of the regional state of stress in a jointed rock mass.

As the above study illustrates, the numerical model should be able to simulate both the presence of the geologic structure and the loading path to calculate this heterogeneous in situ state. The two-dimensional DEM/EFD code UDEC is able to address both of these conditions. UDEC provides a stable solution for the physical instabilities that develop as a result of joint slippage or separation during the load cycle.

The DEM analysis can also be extended to evaluate the effects of the localized locking-in of stress concentrations along the length of the discontinuity in addition to concentrations initiating at crack tips. In this case, the

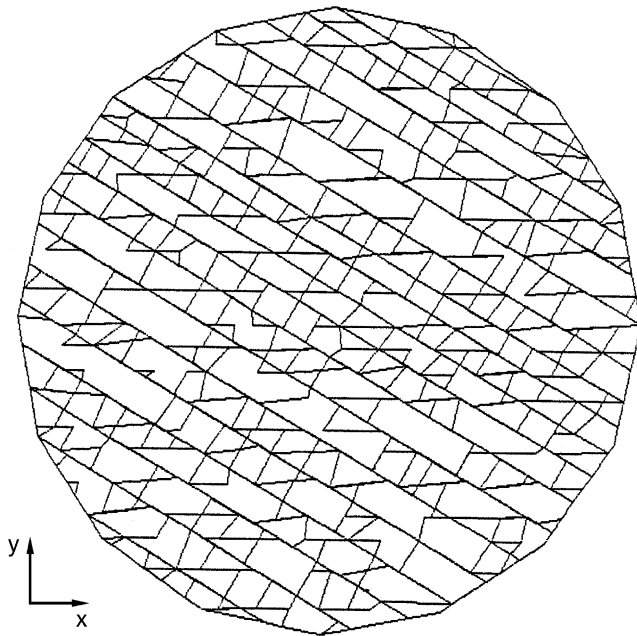


Fig. 4. Jointed rock mass defined by one set of continuous joints and two sets of discontinuous joints (from [20]).

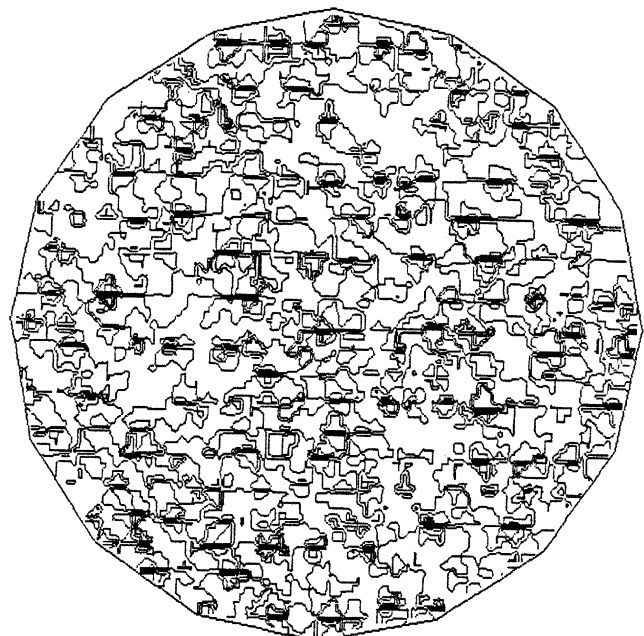


Fig. 5. Contours of  $\sigma_{xx}$  after one cycle of loading (from [20]).

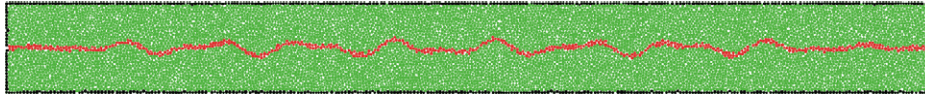


Fig. 6. PFC2D model of joint (represented by unbonded particles, shown in red) subjected to shear loading. Upper and lower sets of velocity-controlled particles are shown in black (from [21]).

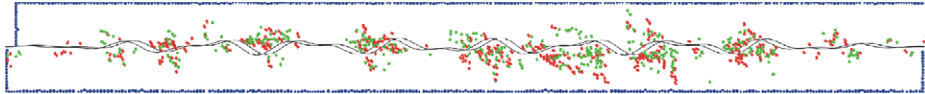


Fig. 7. Localized tensile and shear failure along joints identified by microcracks resulting from shear displacement: red denotes tension failure; green denotes shear failure (from [21]).

stress concentrations are related to the physical roughness of the joint. For example, DEM particle codes have been applied to represent the roughness profile of a joint explicitly. Cundall [21] describes numerical shear tests on rough joints using the particle code PFC2D. Fig. 6 shows one model from this study. The model represents a rock sample as a collection of bonded particles. All contacts are bonded except those corresponding to the “joint” to be tested. The joint location, indicated by the red balls in Fig. 6, is defined by a given roughness profile. Shear tests were then conducted on this model. This representation of a rough joint in rock results in simulated behavior that is similar to that observed for real joints. For example, Fig. 7 presents one result in which localized tensile and shear failures are found to develop, and the extent of the damage locations are shown to be related to the locations of joint asperities. One observation was that tensile cracking is predominant at low normal stress, and shear failure is predominant at high normal stress. The development of these localized damage zones along the joint can be expected to influence the development of stress concentrations in the vicinity of the joint.

## 5. Correlation of acoustic emission/microseismic data to stress state

One of the promising advances to determine stress-field information is the approach employing acoustic monitoring. Microseismic monitoring systems can be used to identify regions in the rock mass with greater potential for rock fracture, and this information can then be correlated to stress concentrations in the rock mass. For example, regions of stress concentrations have been shown to coincide with regions of high-velocity anomalies, which can be identified by passive tomographic imaging. The high-stress regions are identified by increased potential for rock fracturing. Further, waveform processing from microseismic investigations can provide information on the principal stress orientation at the acoustic source. See [22] for descriptions of microseismic investigations.

Recently, a new method has been proposed to estimate in situ principal stresses in the horizontal direction based on acoustic emission testing of rock core in the laboratory; e.g. see [23,24]. This method is based on the “Kaiser effect”, which indicates that rocks exhibit “stress memory.” Kaiser [25] observed that acoustic emissions in rock specimens subjected to cyclic uniaxial loading occurred only after the previously experienced maximum stress was re-established. For additional discussion of the Kaiser effect, also see [26]. This discovery is applied by these researchers to define a three-dimensional “damage surface” from tests on rock core; this surface defines the state at which acoustic emissions commence. A damage-surface locus is developed by plotting the onset points of acoustic emission for different applied horizontal stress magnitudes. The shape of the damage-surface points plotted on a major–minor horizontal stress plot is shown by Pestman et al. [23] to provide an estimate for the maximum in situ horizontal stress state experienced during coring. The maximum curvature in the plot (i.e. the location of a “knee” in the plot) denotes the stress state during coring.

Numerical modeling can play an important role in checking and collaborating stress estimation techniques, such as the types described above. By integrating microseismic investigations with explicit, dynamic numerical modeling, it is possible to develop new insights in understanding the in situ stress state and validate the potential of these investigations.

A powerful feature of explicit, dynamic DEM codes is the ability to simulate acoustic emission and microseismic activity directly. In particular, particle codes, such as PFC2D and PFC3D, can be shown to produce breakage of contact bonds that can be correlated to microseismic activity; see [27]. In fact, Hazzard and Young [28] have developed algorithms to correlate “clusters” of particles, whose bonds break within a given space and time, to larger-magnitude events.

The simulation of microseismic events in the particle code is performed in the following manner. If the stresses applied to a particle model cause the forces at particle contact bonds to exceed the bond strength, then



the bonds will break. Consequently, some of the strain energy stored at the contact will be released as kinetic energy, which will travel through the model as a seismic wave. These waves can be monitored and compared to seismic energy that would be recorded in a microseismic investigation. A direct comparison between bond breakage in the model and acoustic emissions may be hard to achieve, as the type and size of the source mechanism and the properties affecting wave propagation can be difficult to represent in the model. Nevertheless, correlations can be made. For example, see Hazzard et al. [29] for comparison of particle code seismic parameters to those obtained by acoustic emission information.

Studies have demonstrated the ability of particle codes to simulate stress memory; e.g. see [30,31]. A PFC3D model was applied to simulate the various stages of extracting a rock core, releasing the stresses during coring and reloading in the laboratory. Fig. 8 plots stress levels and bond breakage rates from the PFC3D simulation versus experimental time. The plot indicates that bonds break initially during unloading (coring), which results in core damage. Then, when the sample is reloaded, there is no initial activity. The onset of bond breakage during reloading occurs when the previous state of stress is reached.

Holt et al. [32] report the results of PFC3D simulations in which the sample is subjected to multiple reloading stress paths in the horizontal direction to develop a damage-surface plot similar to that reported by Pestman et al. [23] from laboratory tests. Fig. 9 shows the plot developed from the PFC3D experiments. The “knee” in this plot is shown to correspond to the original in situ stress state chosen for this model.

These numerical experiments indicate the potential of numerical models to add insight into understanding the effects of rock fracturing on the state of stress. Further, as illustrated above, these models may be able to form the basis for developing practical methods to use the

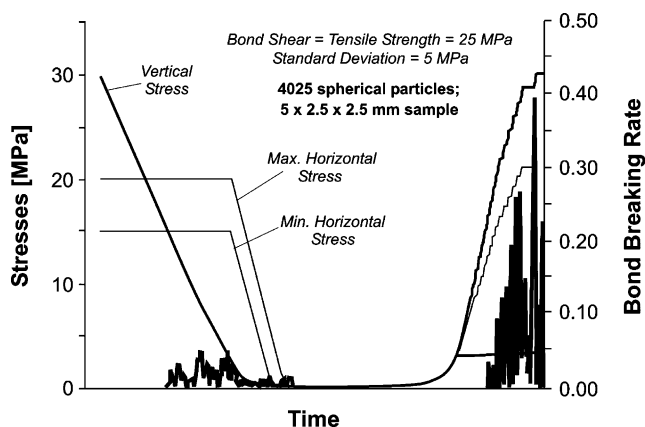


Fig. 8. Stress and bond breakage rate versus experiment time for PFC3D simulation (from [31]).

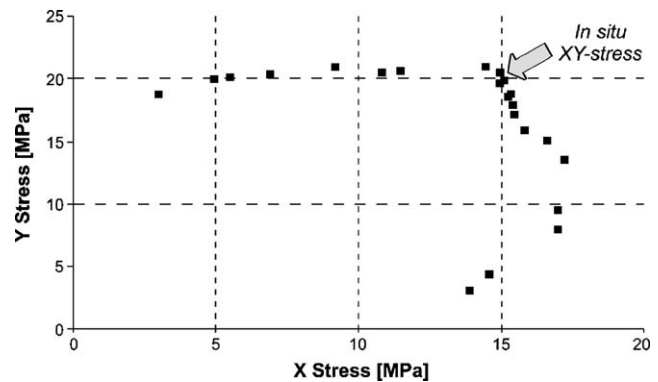


Fig. 9. Damage surface in the horizontal plane from PFC3D simulations (from [32]).

microseismic investigations, both in the field and laboratory, to derive information related to the in situ stress field.

## 6. Future development

Most numerical studies of the effects of conditions (in particular, geologic structure and rock fracturing) on in situ stresses are two-dimensional. Clearly, the influence of geologic structure and the effect of microseismic activity are three-dimensional, and three-dimensional models should be used to represent the rock mass adequately to evaluate these effects on the stress state. At present, the use of 3D explicit, dynamic-solution DEM models is limited by the memory capacity and calculation-time restrictions of today's personal computers. However, as Cundall [33] contends, this restriction should be greatly alleviated within the next 10–20 years, and the application of 3D DEM models to incorporate sufficient details in the evaluation of in situ stress states should become more viable.

Even with significant advancements in computing power, large-scale regional DEM models of a rock mass, on the scale shown in Figs. 2 and 3, may still require extremely computer-intensive memory capacity and calculation times. One solution that has been proposed recently is the use of an “adaptive continuum/discontinuum” modeling approach. With this approach, calculations are made more economical by replacing regions in the DEM model, which do not have discontinuities, with an elastic continuum formulation. Further, this approach may be automated such that these regions may switch from the elastic formulation to the particle representation automatically when some pre-defined stress level is reached locally in the model. The particle representation then would simulate the effects associated with rock fractures more accurately. The viability of this adaptive modeling approach is currently under investigation [34].



## References

- [1] Jing L. A review of techniques advances and outstanding issues in numerical modelling for rock mechanics and rock engineering. *Int J Rock Mech Min Sci* 2003;40(3):283–353.
- [2] Cundall PA. Explicit finite-difference methods in geomechanics. In: *Proceedings of the ASCE Engineering Federation Conference on Numerical Methods in Geomechanics*, Virginia, June 1976. p. 132–50.
- [3] Cundall PA, Strack ODL. A discrete numerical model for granular assemblies. *Géotechnique* 1979;29:47–65.
- [4] Cundall PA. A computer model for simulating progressive large scale movements in block rock systems. In: *Symposium of the International Society of Rock Mechanics*, Nancy, France, Paper II.8, 1971.
- [5] Cundall PA. Rational design of tunnel supports: a computer model for rock mass behaviour using interactive computer graphics for the input and output of geometrical data. *US Army Corps of Engineers, Missouri River Division, Technical report MRD-2-74*, 1974.
- [6] Itasca Consulting Group Inc. *FLAC (Fast Lagrangian Analysis of Continua) version 4.0*. Minneapolis: ICG; 2000.
- [7] Itasca Consulting Group Inc. *FLAC3D (Fast Lagrangian Analysis of Continua in 3 Dimensions) version 2.1*. Minneapolis: ICG; 2002.
- [8] Itasca Consulting Group Inc. *PFC2D (Particle Flow Code in 2 Dimensions) version 3.0*. Minneapolis: ICG; 2002.
- [9] Itasca Consulting Group Inc. *PFC3D (Particle Flow Code in 3 Dimensions) version 2.0*. Minneapolis: ICG; 1999.
- [10] Itasca Consulting Group Inc. *UDEC (Universal Distinct Element Code) version 3.1*. Minneapolis: ICG; 2000.
- [11] Itasca Consulting Group Inc. *3DEC (3 Dimensional Distinct Element Code) version 2.0*. Minneapolis: ICG; 1998.
- [12] McKinnon SD. Analysis of stress measurements using a numerical model methodology. *Int J Rock Mech Min Sci* 2001;38:699–709.
- [13] Konietzky H, Blümling P, Rummel F. In situ stress field in the Wellenberg area. *NAGRA Bull* 1995;26:38–48.
- [14] Carranza-Torres C, Brandshaug T, Damjanac B. Regional and local scale thermal-mechanical analysis of the rock mass surrounding waste emplacement drifts at Yucca Mountain (draft report). Las Vegas: BSC; April 2002.
- [15] McKinnon SD, Lorig LJ. Considerations for three-dimensional modelling in analysis of underground excavations. In: Sharma VM, Saxena KR, Woods RD, editors. *Distinct element modelling in geomechanics*. New Delhi: Oxford & IBH Publishing; 1999. p. 145–66.
- [16] Brox DR, Konietzky H, Rummel F. In situ stress measurements using hydraulic fracturing in jointed rock in Hong Kong. In: *Geotechnical rise—identification, evaluation and solutions (Proceeding of the Sixth Australia–New Zealand Conference on Geomechanics, Christchurch, February)*. Christchurch: New Zealand Geomechanics Society; 1992. p. 213–35.
- [17] Mayeur B, Fabre D. Measurement and modelling of in situ rock stresses in the Ambin Massif, Franco-Italian Alps. In: Amadei B, Kronz RL, Scott GA, Smeallie PH, editors. *Rock mechanics for industry*, vol. 2 (Proceedings of the 37th US Rock Mechanics Symposium, Vail, Colorado, June 1999). Rotterdam: Balkema; 1999. p. 1157–63.
- [18] Brady BHG, Friday RC, Alexander LG. Stress measurement in a bored raise at the Mount Isa Mine. In: *Proceedings of the International Society on Rock Mechanics Symposium on Investigation of Stress in Rock*. Sydney: Institute of Engineers Australia; 1976. p. 12–6.
- [19] Knott JF. *Fundamentals of fracture mechanics*. London: Butterworths; 1973.
- [20] Brady BHG, Lemos JV, Cundall PA. Stress measurement schemes for jointed and fractured rock. In: *Proceedings of the International Symposium on Rock Stress and Rock Stress Measurements*, Stockholm. Luleå: Centek Publishers; 1986. p. 167–76.
- [21] Cundall PA. Numerical experiments on rough joints in shear using a bonded particle model. In: Lehner FK, Urai JL, editors. *Aspects of tectonic faulting (Festschrift in Honour of George Mandl)*. Berlin: Springer; 2000. p. 1–9.
- [22] Young RP, Baker C. Microseismic investigation of rock fracture and its application in rock and petroleum engineering. *ISRM News J* 2001;7(1):19–27.
- [23] Pestman BJ, Kenter CJ, van Munster JG. Core-based determination of in-situ stress magnitudes. In: Elsworth, Tinucci, Heasley, editors. *Rock mechanics in the national interest*, vol. 2 (Proceedings of the 38th US Rock Mechanics Symposium, Washington, DC, July 2001). Lisse: Swets & Zeitlinger; 2001. p. 1353–60.
- [24] Pestman BJ, Holt RM, van Munster JG, Kenter JG, Field CJ. Field application of a novel core-based in-situ stress estimation technique. *OilRock* 2002, SPE/ISRM 78158.
- [25] Kaiser J. Erkenntnisse und folgerungen aus der messung von gerauschen bei zugbeanspruchung von metallischen werkstoffe. *Arch Eisenhüttenwesen* 1953;24:23–4.
- [26] Lavrov A. The Kaiser effect in rocks: principles and stress estimation techniques. *Int J Rock Mech Min Sci* 2003;40(2): 151–71.
- [27] Hazzard JF, Young RP. Seismic validation of micromechanical models. In: Elsworth, Tinucci, Heasley, editors. *Rock mechanics in the national interest*, vol. 2 (Proceedings of the 38th US Rock Mechanics Symposium, Washington, DC, July 2001). Lisse: Swets & Zeitlinger; 2001. p. 1029–34.
- [28] Hazzard JF, Young RP. Simulating acoustic emissions in bonded-particle models of rock. *Int J Rock Mech Min Sci* 2000;37(5): 867–72.
- [29] Hazzard JF, Maxwell SC, Young RP. Micro-mechanical modelling of acoustic emissions. In: *EUROCK 98*, vol. 2 (Proceeding of the SPE/ISRM Conference on Rock Mechanics in Petrol Engineering, Trondheim, July 1998). Richardson, Texas: SPE; 1998. p. 509–17.
- [30] Holt RM, Brandshaug T, Cundall PA. Discrete particle and laboratory modelling of core mechanics. In: Girard, Liebman, Breeds, Doe, editors. *Pacific rocks 2000: rock around the rim (Proceeding of the Fourth North American Rock Mechanics Symposium, Seattle, July–August 2000)*. Rotterdam: Balkema; 2000. p. 1217–24.
- [31] Holt RM, Pestman BJ, Kenter CJ. Use of a discrete particle model to assess feasibility of core based stress determination. In: Elsworth, Tinucci, Heasley, editors. *Rock mechanics in the national interest*, vol. 2 (Proceeding of the 38th US Rock Mechanics Symposium, Washington, DC, July 2001). Lisse: Swets & Zeitlinger; 2001. 1361–6.
- [32] Holt RM, Doornhof D, Kenter CJ. Use of discrete particle modeling to understand stress-release effects on mechanical and petrophysical behavior of granular rocks. In: Konietzky H, editor. *Numerical modeling in micromechanics via particle methods*. Lisse: Swets & Zeitlinger; 2003. p. 269–76.
- [33] Cundall PA. A discontinuous future for numerical modelling in geomechanics? *Geotech Eng* 2001;149(1):41–7.
- [34] Cundall PA, Ruest MR, Guest AR, Chitombo G. Evaluation of schemes to improve the efficiency of a complete model of blasting and rock fracture. In: Konietzky H, editor. *Numerical modelling in micromechanics via particle methods*. Lisse: Swets & Zeitlinger; 2003. p. 107–15.